Chemical Engineering Journal 146 (2009) 428–433

Contents lists available at ScienceDirect

Chemical Engineering Journal

journal homepage: www.elsevier.com/locate/cej

Gas–liquid flow in T-junction microfluidic devices with a new perpendicular rupturing flow route

J. Tan, S.W. Li, K. Wang, G.S. Luo*

The State Key Lab of Chemical Engineering, Department of Chemical Engineering, Tsinghua University, Beijing 100084, China

ARTICLE INFO

Article history:
Received 16 June 2008
Received in revised form
24 September 2008
Accepted 8 October 2008

Keywords:
Microfluidic
T-junction
Angle of intersection
Monodisperse

ABSTRACT

In this paper a series of perpendicular rupturing flow routes with differing angles ranging from 30° to 150° between the entrance channels were used to control the gas–liquid phase dispersed flow in T-junction microfluidic devices. Uniform gas bubble plugs were produced in consistent, two-phase flows within the channels of the microfluidic devices. Both the gas–liquid flow and the size of the gas bubbles, which ranged from 800 to 3100 μm in length, depended on several influential factors including the flow rates, the physical properties of the liquid phase, and the angle between entrance channels. Considering these factors and the equilibrium between the shear force and interfacial tension within the microfluidic channels, an equation was derived in the form of $L/w = 1/2(Q_G/Q_L \sin\theta + 2/5 \cot\theta)^{1/2} Ca^{-1/5}$ relating the angle between the entrance channels of the two phases to the gas bubble plug length within the microfluidic device. The relationship allows for the prediction of gas bubble plug length in T-junction microfluidic devices employing intersection angles ranging from 30° to 150° and is thus potentially useful for the controllable preparation of monodisperse gas bubbles.

1. Introduction

Micro-sized bubbles have recently caught the attention of many researchers for their numerous and diverse applications to expanding scientific fields and emerging technologies. Microbubbles have already shown great potential as ultrasound contrast agents, therapies for thrombus destruction, and new targeted drug delivery and flotation column methods [1–4]. In all of these applications, the bubble size and distribution are important parameters.

Similarly, microfluidic devices have also gained the attention of many researchers in the past several years for their application to on-chip separations [5–7], kinetic analysis [8,9], and protein crystallization [10,11]. These devices, and the exact control of small volumes of fluids and understanding of multiphase flows which they require, make them potentially suitable systems for monodisperse gas bubble production.

In the past, dispersions in liquid–liquid systems have been achieved using several different methods including geometry-dominated break-up [12], hydrodynamic flow focusing through a small orifice [13,14], and two-phase cross-flowing rupture streams in T-junction microfluidic devices [11,15–19]. The mechanisms in all these methods are primarily driven by the drag force of the continuous phase and the momentum of the dispersed phase, and past studies have investigated the effects of parameters such as flow rate, viscosity and interfacial tension on these forces. Many recent studies have also focused on gas–liquid dispersions in microfluidic devices. Ganan-Calvo et al. [20–22] described the formation of monodisperse gas bubbles using a hydrodynamic flow focusing method through capillaries and orifices. Garstecki et al. [23,24] produced monodisperse bubbles with frequencies exceeding 10^5 bubbles per second by using a flow focusing devices and found that the volume of the bubbles, V_b, scaled with the flow rate of the gas stream, Q_G, and the flow rate of the liquid stream, Q_L, according to the relationship $V_b \propto Q_G/Q_L$. Xu et al. [25] prepared monodisperse microbubbles using a cross-flowing shear-rupturing technique in a T-junction microfluidic device and found the diameter of the bubbles scaled with the liquid flow rate, u_L, and the liquid viscosity, μ_L, as $d_b \propto 1/u_G\mu_L$. Yasuno et al. [26] described the formation of monodisperse microbubbles using a geometry-dominated breakup method on a microchannel plate. Their study showed that the bubble/plug size was mainly affected by the operating conditions and the physical properties including surface/interfacial tension and continuous phase viscosity.

In our previous work, uniform liquid plugs were produced using a cross-junction microfluidic device, and a controlled preparation of monodisperse emulsions was achieved with a new perpendicular rupturing channel [27]. The mechanisms controlling the formation of plug flow have been thoroughly discussed, and a quantitative equation has been developed to predict the plug length. Considering the comparability between gas–liquid and

* Corresponding author. Tel.: +86 10 62783870; fax: +86 10 62783870.
E-mail address: gsluo@tsinghua.edu.cn (G.S. Luo).

1385-8947/$ – see front matter © 2008 Elsevier B.V. All rights reserved.
doi:10.1016/j.cej.2008.10.024

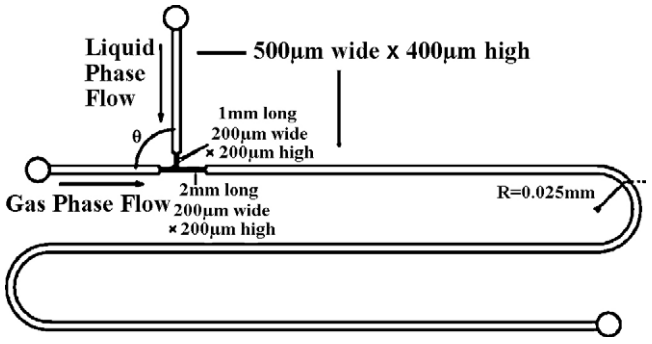

Fig. 1. The T-junction microfluidic device with intersection angle θ.

liquid–liquid systems, we introduced the new perpendicular rupturing flow channel into T-junction microfluidic devices to produce uniform gas-plug flow in water. In addition, an improved T-junction microfluidic device was designed to maintain a more stable gas stream pressure at the intersection of the two fluids. T-junction microfluidic devices with different angles of intersection were used to form gas-plug-in-water dispersion flow, and the influence of the angle of intersection between the two entrance channels on plug length was investigated. Here, we also discuss the mechanisms behind the formation of gas-plug-in-water flow and propose a quantitative equation developed to predict the gas plug length.

2. Experimental

2.1. Microfluidic device

T-junction microfluidic devices with differing angles of intersection were fabricated on a 60 mm × 40 mm × 3 mm polymethyl methacrylate (PMMA) plate using an end mill. Both the straight and intersecting channels were 500 μm wide × 400 μm high. At the intersection, both channels become narrower, 200 μm wide × 200 μm high, with the narrow section on the intersecting channel 1 mm in length and the narrow section on the straight channel 3 mm in length (Fig. 1). The microfluidic devices were sealed using another 1 mm thick PMMA plate cured at 105 °C using high-pressure thermal sealing techniques. Two microsyringe pumps were used to pump the two phases into the two flow channels. The liquid phase was pumped into the intersecting channel. Fig. 2 shows photos of the T-junction microfluidic devices.

2.2. Materials

Air at 20 °C was used for the gas phase. Aqueous solutions with 0, 15, 24, 30, 35 wt.% glycerol were used as the liquid phases. Either SDS or Tween 20 at 1 wt.% concentration was used as the water-soluble surfactant added to the liquid phase.

Glycerol, SDS and Tween 20 used in the experiment were analytically pure and purchased from Beijing Chemical Plant.

2.3. Apparatus and analysis

The surface tension was measured with the pendant drop technique using a DataPhysics Instruments GmbH (Filderstadt). Experiments were carried out with a microscope at 40× magnification. A high-speed CCD video camera was connected to the microscope and images were recorded at a frequency of 200 images/s. The lengths of the plugs were measured from the microscope images and after changing any of the flow parameters, 100 s of equilibration time was observed.

3. Results and discussion

3.1. Gas–liquid flow in the T-junction microfluidic device with perpendicular rupturing

In our previous study, we examined a new flow channel route, which utilizes a perpendicular shear force induced break-up to produce monodisperse droplets in a T-junction microfluidic device. The device employs a quartzose capillary embedded into the perpendicular channel as the water-phase flow channel [19]. Using this system, we prepared oil-in-water (O/W) and water-in-oil (W/O) emulsions in a symmetrical cross-junction microchannel [27]. In this study, we examined gas–liquid flow in the T-junction microfluidic devices with different intersecting angles between the two entrance channels by adding a surfactant into the liquid phase.

Ordered gas-plug flow was achieved when SDS was added, decreasing the surface tension from 72.75 to 27.15 mN/m. Consistent two-phase flow occurred only sporadically if SDS was not added to the system. We also tested the microfluidic devices without narrower channels near the intersections and found that the gas plugs formed were non-uniform because of the instability of the pressure at the intersection. Thus, with these modifications, ordered gas-plug flow with polydispersity index values of less than 2% was achieved.

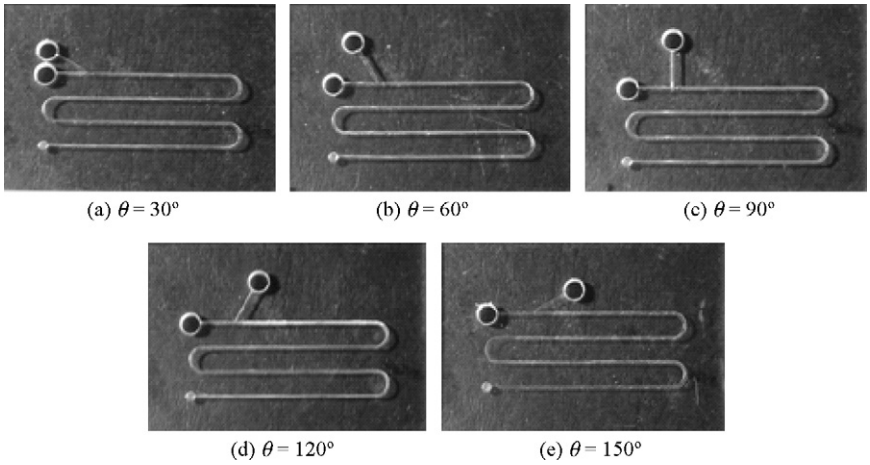

Fig. 2. T-junction microfluidic devices with different angles.

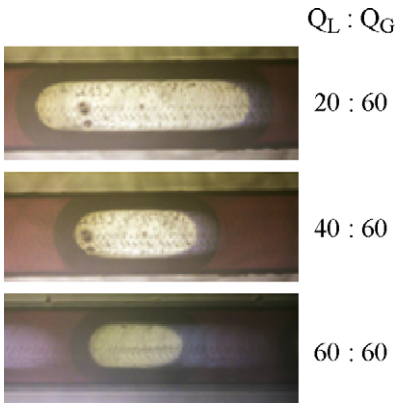

Fig. 3. Micrographs illustrating the influence of the gas phase flow rate on gas plug length.

Our prior research also indicated that the size of the dispersed phase is independent of the surfactant concentration when the surfactant concentration is higher than the critical micelle concentration (C_{mc}) [27]. In these experiments, the surfactant concentration was higher than C_{mc}, which was 9.7 mmol/L for SDS [28].

Other parameters were also investigated to determine their influence on gas plug length. Fig. 3 shows the micrographs of gas plugs under different liquid phase flow rates with a fixed gas phase flow rate of 60 μL/min. Fig. 4 shows the effect of different flow rates on gas plug length. As shown in Fig. 4, the gas plug length increases as the gas phase flow rate increases, and decreases as the liquid phase flow rate increases. However, the gas plug length at Q_L = 60 μL/min slightly decreases when the gas phase rate increases to 140 μL/min. This phenomenon is probably caused by the instability of the two-phase interface as the shear force increases, as reported in the literature [29]. However, the data in the unstable region is not considered in this work and will be addressed in further research.

Aqueous solutions with 0, 15, 24, 30, 35 wt.% glycerol were used to determine the effect of the viscosity of the liquid phase on gas plug length at a fixed liquid phase rate of 20 μL/min. As shown in Fig. 5, the gas plug length decreases with the increase of the liquid phase viscosity, μ, while the change of surfacial tension is unobvious, as shown in Table 1.

Tween 20 was used as the surfactant to determine the effect of the liquid phase surface tension on gas plug length at a liquid phase flow rate of 40 μL/min. The concentration of Tween 20 was 1 wt.%, higher than its C_{mc} value of 0.028 mmol/L [30]. As shown in Fig. 6, the gas plug length increases with the increase of the surface

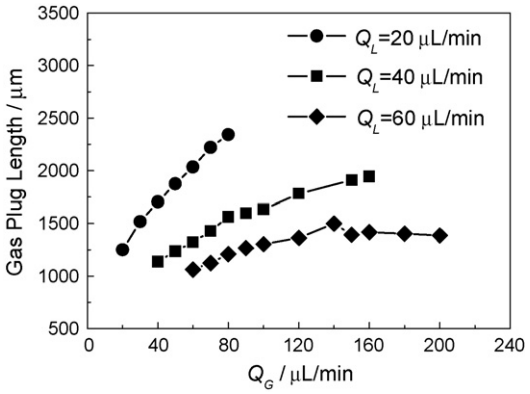

Fig. 4. Influences of two-phase flow rates on gas plug length.

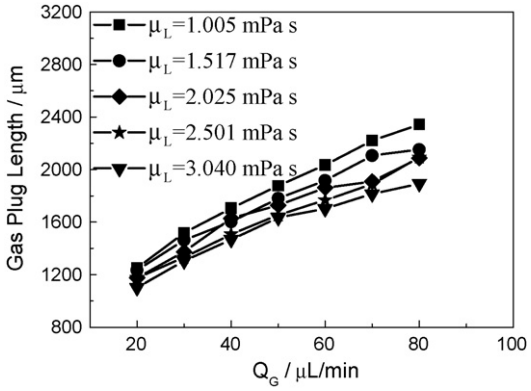

Fig. 5. Influence of liquid phase viscosity on gas plug length, Q_L = 20 μL/min.

Table 1
Viscosity and surfacial tension of aqueous solutions with different glycerol concentration.

Glycerol concentration (wt.%)	Viscosity of solution (mPa s)	Surfacial tension of solution (mN/m)
15	1.517	32.98
24	2.025	34.08
30	2.501	32.85
35	3.040	35.11

tension of the liquid phase, γ.

As shown above, the gas plug length decreases with the increase in the velocity and viscosity of the liquid phase, while it increases with the increase in the velocity of the gas phase and the surface tension of the liquid phase. These results are similar to those from the symmetrically perpendicular rupturing in the cross-junction microfluidic device [27]. By considering the equilibrium between shear force of the continuous flow and interfacial tension, and the influence of the two-phase flow ratio on the shape of the interface, the plug length could be expressed by (Eq. (1)) as

$$\frac{L}{w} = k\left(\frac{Q_d}{Q_c}\right)^{\alpha} Ca^{\beta} \quad (1)$$

where L is the dispersed phase plug length, w is the width of the microchannel, Q_c is the continuous phase flow rate, Q_d is the dispersed phase flow rate, and Ca is the capillary number defined as $Ca = u_c\mu/\gamma$.

Considering the comparability of the plug formation mechanisms in the symmetrical and asymmetrical cross-junction microchannels, we used (Eq. (1)) to predict the gas plug length in

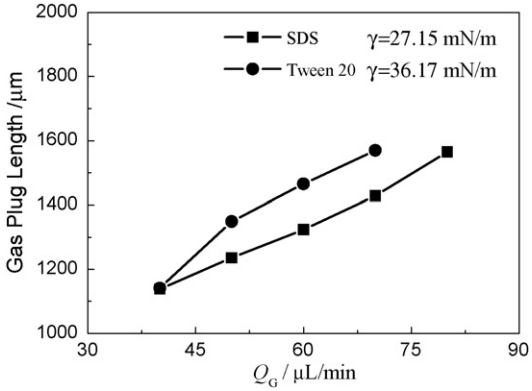

Fig. 6. Influence of the liquid phase surface tension on gas plug length, Q_L = 40 μL/min.

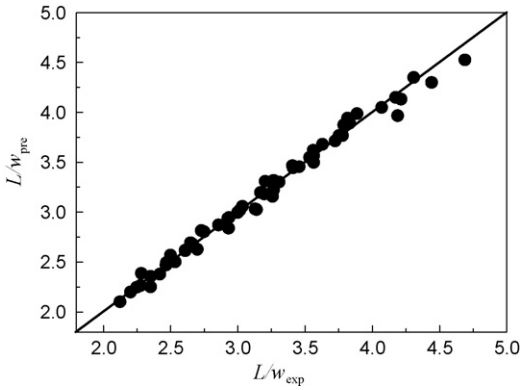

Fig. 7. Comparison between correlated values and experimental data.

the new T-junction microfluidic devices as well and a linear regression was used to evaluate the data. The equation for the calculation of the plug length was thus

$$\frac{L}{w} = \frac{1}{2}\left(\frac{Q_G}{Q_L}\right)^{1/2} Ca^{-1/5} \quad (2)$$

where Q_G is the gas phase flow rate, Q_L is the liquid phase flow rate, and Ca is defined as $Ca = u_L\mu/\gamma$, where u_L is the velocity of liquid phase in the main straight channel. This correlation equation appeared to provide a good fit across the entire range of data collected from the experiments, as shown in Fig. 7.

Comparing (Eq. (2)) with the previous result for liquid–liquid dispersed flow in symmetrical cross-junction microfluidic device [27], $L/w = 8/5(Q_d/Q_c)^{1/5}Ca^{-1/5}$, we found out that the power of the capillary number, β, which characterizes the equilibrium between shear force of the continuous flow and the interfacial tension, has the same value. This implies that the power of the capillary number, β, is only affected by the main channel and is independent of the different intersecting structures in these types of microfluidic devices. Furthermore, any difference in α, the ratio between the continuous phase and the dispersed phase which characterizes the shape of the interface, should be attributed to a change in the junction of the microfluidic device.

3.2. Gas–liquid flow in T-junction microfluidic devices with different entrance angles

In this series of experiments, we used T-junction microfluidic devices with the entrance channels intersecting at angles of 60° or 120° to realize gas–liquid dispersed flow with uniform gas plugs. Fig. 8 shows the effect of different flow rates on plug length. The gas plug length increases as the gas phase flow rate increases, and decreases as the liquid phase flow rate increases, showing the same trend as the microfluidic devices with a perpendicular intersecting channel. As shown in Table 2, at constant flow rates for both phases, the plug length reaches a minimum value at an intersection angle of 90°. This phenomenon is most likely due to the fact that a maximum rupturing velocity and thus a minimum value for the rupturing time is reached at a 90° angle, resulting in a smaller plug length. As shown in Fig. 9, the entrance channel angle makes the shape of the interface and rupturing time different.

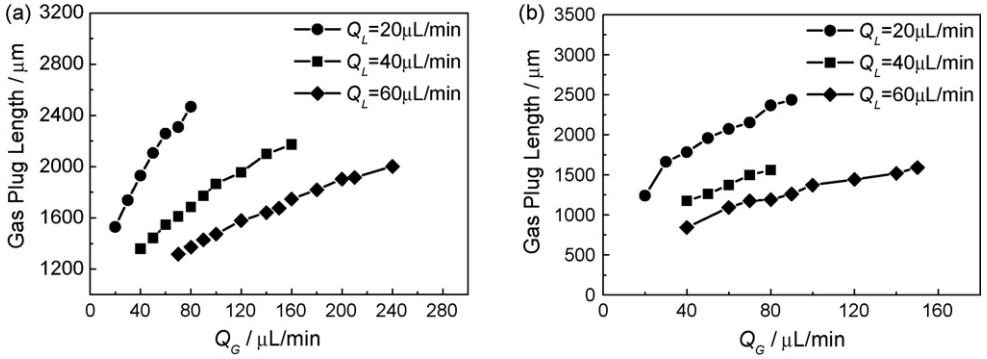

Fig. 8. Influences of two-phase flow rates on plug length. (a) $\theta = 60°$; (b) $\theta = 120°$.

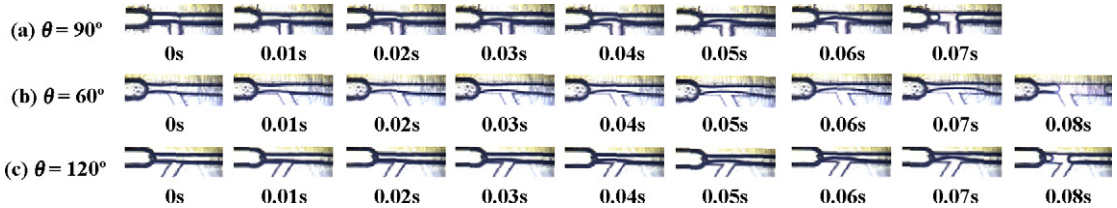

Fig. 9. Images of gas rupture events at different angles. $Q_L = 20$ μL/min, $Q_G = 40$ μL/min.

Table 2
Influence of the entrance angle on plug length.

Entrance angle	Gas plug length (μm)			
	$Q_L = 20$ μL/min, $Q_G = 40$ μL/min	$Q_L = 20$ μL/min, $Q_G = 80$ μL/min	$Q_L = 40$ μL/min, $Q_G = 60$ μL/min	$Q_L = 60$ μL/min, $Q_G = 100$ μL/min
$\theta = 60°$	1930	2468	1547	1473
$\theta = 90°$	1705	2344	1324	1304
$\theta = 120°$	1782	2366	1374	1374

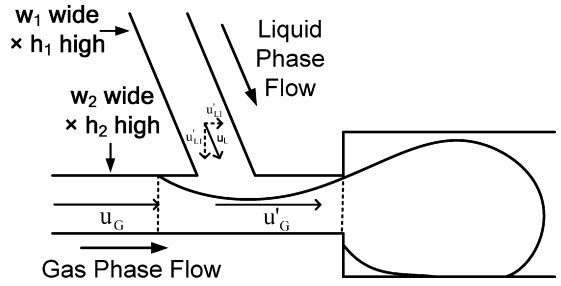

Fig. 10. Sketch of the rupture process of gas plug at the intersection.

Correlations were made by extending the results of the gas plug length experiments in the perpendicular T-junction microfluidic devices to the microfluidic devices with entrance channel intersection angles $\theta = 60^\circ$ and $\theta = 120^\circ$. Both the shape of the interface and the equilibrium between the shear force of the water flow and the surface tension were also considered.

The influence of the interface shape on the gas plug length L_1 was analyzed as follows. The rupturing of the interface causes the formation of the gas plug. As shown in Fig. 10, in the perpendicular T-junction microfluidic device, the gas stream is sheared by the liquid stream with a velocity of $u_L = Q_L/h_1 w_1$ until a gas plug is formed. During the rupture time $t = w_2/u_L$, the volume of gas plug formed should be $V = Q_G t = u_G h_2 w_2 (w_2/u_L)$. Therefore, the influence that the shape of the microfluidic device exerts on gas plug length is proportional as

$$L_1 \propto \frac{u_G}{u_L}$$

We consider the influence of the angle between the two entrance channels on this process in two different aspects. First, the perpendicular velocity required to rupture the plug must be modified to $u'_{L1} = u_L \sin\theta$. However, the influence of the horizontal contribution of the liquid velocity on the gas flow rate in the formation stage should also be considered. For a channel with intersecting angle θ, the horizontal part of the liquid velocity is $u'_{L2} = u_L \cos\theta$. This velocity is co-current with the gas flow when $\theta < 90^\circ$, but counter current with the gas flow when $\theta > 90^\circ$. We assume that the effect of u'_{L2} leads to the modification of the gas velocity as

$$u'_G = u_G + \lambda u_L \cos\theta$$

where λ is an efficiency coefficient, which changes as θ goes from being less than to greater than 90°.

Considering both the horizontal and vertical components of the liquid phase velocity influence of the angle of the intersecting channel, θ, on the plug length can be expressed as

$$L_1 \propto \frac{u'_G}{u'_L} = \frac{u_G + \lambda u_L \cos\theta}{u_L \sin\theta} = \frac{Q_G}{Q_L \sin\theta} + \lambda \cot\theta$$

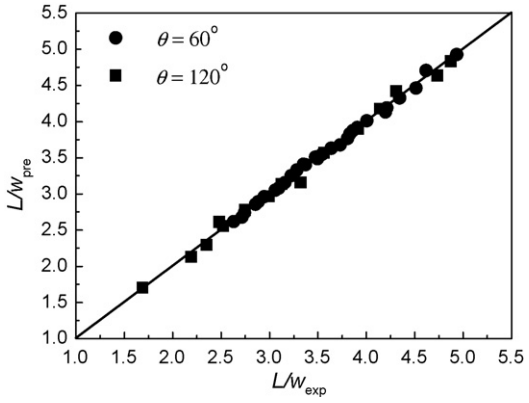

Fig. 11. Comparison between correlated values and experimental data.

Yet another factor affecting the length of gas plug is the equilibrium between the shear force of the water flow and the interfacial tension, which is characterized by the capillary number ($Ca = u_L \mu/\gamma$). The balance between the surface tension and the shear force was considered only in the main channel because the narrow channel is very short, and the water flow velocity is independent of the angle between the two entrance channels. Thus, the liquid velocity u_L used in calculating capillary number Ca has not been modified.

Considering the influence of the entrance angle on both the shape of the interface and the equilibrium between shear force of the liquid flow and the interfacial tension, we assume that the gas plug length could be expressed as

$$\frac{L}{w} = k\left(\frac{Q_G}{Q_L \sin\theta} + \lambda \cot\theta\right)^{\alpha} Ca^{\beta}$$

where the parameters k, α and β are all the same as those determined before using the data in the perpendicular channel.

A linear regression was used to evaluate the parameters λ_1 and λ_2 in T-junction microfluidic devices with intersecting angles $\theta = 60^\circ$ and $\theta = 120^\circ$, respectively. The regression showed that $\lambda_1 = \lambda_2 = 0.4$.

The gas plug length formed in a T-junction microfluidic device with angle θ was then predicted using (Eq. (3)).

$$\frac{L}{w} = \frac{1}{2}\left(\frac{Q_G}{Q_L \sin\theta} + \frac{2}{5}\cot\theta\right)^{1/2} Ca^{-1/5} \quad (3)$$

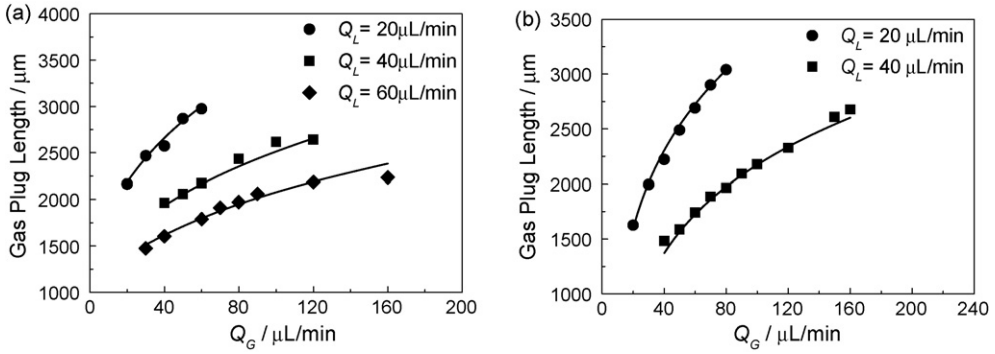

Fig. 12. Comparison between experiment data and predicted data. (a) $\theta = 30^\circ$; (b) $\theta = 150^\circ$.

The correlation equation provided a good fit across the entire range of data, as shown in Fig. 11.

3.3. Further verification of the model

To further verify the experimental results, gas–liquid dispersed flow was also examined in T-junction microfluidic devices with intersection angles $\theta = 30^\circ$ and $\theta = 150^\circ$. Fig. 12 shows the close agreement in the comparison between the experimental data and the predicted results.

4. Conclusions

In this paper, we introduced a new perpendicular rupturing flow route to control the gas–liquid dispersed flow in T-junction microfluidic devices with different angles of intersection between the two entrance channels. The microfluidic system was modified by adding a surfactant to the water phase and by making the channels at the intersection of the T-junction microfluidic devices more narrow. The two-phase flow patterns were dependent on the flow rates of both the continuous phase and the dispersed phase. In the perpendicular T-junction microfluidic device, the gas plug length decreased with the increase of the velocity and viscosity of the liquid phase, whereas it increased with the increase of the velocity of the gas phase and the surface tension of the liquid phase. The gas plug length was predicted using the equation $L/w = 1/2(Q_d/Q_c)^{1/2}Ca^{-1/5}$. Considering the influence of the angle between the entrance channels, θ, on the interface shape and the equilibrium between the shear force of the water flow and the interfacial tension, modifications were proposed to extend the equation's prediction capability to T-junction microfluidic devices with different, non-perpendicular intersecting angles ranging from 30° to 150°. The gas plug length in microfluidic devices with intersecting angles $\theta = 60^\circ$ and $\theta = 120^\circ$ was expressed as $L/w = 1/2(Q_G/Q_L \sin\theta + 2/5 \cot\theta)^{1/2}Ca^{-1/5}$. This model provided a good fit across the entire range of experimental data. The extended equation also provided a good prediction for the gas plug length in microfluidic devices with intersecting angles $\theta = 30^\circ$ and $\theta = 150^\circ$. The equation can thus potentially be useful in achieving a more precisely controlled preparation of monodisperse gas bubbles.

Acknowledgments

We would like to acknowledge the support of the National Natural Science Foundation of China (20476050, 20490200, and 20525622) and National Basic Research Program of China (2007CB714302) for this work.

References

[1] D.M. Skyba, S. Kaul, Advances in microbubble technology, Coron. Artery Dis. 11 (2000) 211–219.
[2] M.W. Grinstaff, K.S. Suslick, Air-filled proteinaceous microbubbles: synthesis of an echo-contrast agent, Proc. Natl. Acad. Sci. U.S.A. 88 (1991) 7708–7710.
[3] J.W. Choung, G.H. Luttrell, R.H. Yoon, Characterization of operating parameters in the cleaning zone of microbubble column flotation, Int. J. Miner. Process. 39 (1993) 31–40.
[4] B. Li, D. Tao, Z. Ou, J. Liu, Cyclo-microbubble column flotation of fine coal, Sep. Sci. Technol. 38 (2003) 1125–1140.
[5] A.Y. Fu, C. Spence, A. Scherer, F.H. Arnold, S.R. Quake, A microfabricated fluorescence-activated cell sorter, Nat. Biotechnol. 17 (1999) 1109–1111.
[6] J.D. Ramsey, S.C. Jacobson, C.T. Culbertson, J.M. Ramsey, High-efficiency, two-dimensional separations of protein digests on microfluidic devices, Anal. Chem. 75 (2003) 3758–3764.
[7] X.X. Chen, H.K. Wu, C.D. Mao, G.M. Whitesides, A prototype two-dimensional capillary electrophoresis system fabricated in poly(dimethylsiloxane), Anal. Chem. 74 (2002) 1772–1778.
[8] H. Song, R.F. Ismagilov, Millisecond kinetics on a microfluidic chip using nanoliters of reagents, J. Am. Chem. Soc. 125 (2003) 14613–14619.
[9] G.H. Seong, J. Heo, R.M. Crooks, Measurement of enzyme kinetics using a continuous-flow microfluidic system, Anal. Chem. 75 (2003) 3161–3167.
[10] C.L. Hansen, E. Skordalakes, J.M. Berger, S.R. Quake, A robust and scalable microfluidic metering method that allows protein crystal growth by free interface diffusion, Proc. Natl. Acad. Sci. U.S.A. 99 (2002) 16531–16536.
[11] B. Zheng, L.S. Roach, R.F. Ismagilov, Screening of protein crystallization conditions on a microfluidic chip using nanoliter-size droplets, J. Am. Chem. Soc. 125 (2003) 11170–11171.
[12] S. Sugiura, M. Nakajima, S. Iwamoto, S. Seki, Interfacial tension driven monodispersed droplet formation from microfabricated channel array, Langmuir 17 (2001) 5562–5566.
[13] S.L. Anna, N. Bontoux, H.A. Stone, Formation of dispersions using "flow focusing" in microchannels, Appl. Phys. Lett. 82 (3) (2003) 364–366 (Appl. Phys. Lett.).
[14] Q. Xu, M. Nakajima, The generation of highly monodisperse droplets through the breakup of hydrodynamically focused microthread in a microfluidic device, Appl. Phys. Lett. 85 (2004) 3726–3728.
[15] J.R. Burns, C. Ramshaw, The intensification of rapid reactions in multiphase systems using slug flow in capillaries, Lab. Chip 1 (2001) 10–15.
[16] T. Thorsen, R.W. Roberts, F.H. Arnold, S.R. Quake, Dynamic pattern formation in a vesicle-generating microfluidic device, Phys. Rev. Lett. 86 (2001) 4163–4166.
[17] R. Dreyfus, P. Tabeling, H. Willaime, Ordered and disordered patterns in two-phase flows in microchannels, Phys. Rev. Lett. 90 (2003) 144505.
[18] T. Nisisako, T. Torii, T. Higuchi, Droplet formation in a microchannel network, Lab. Chip 2 (2002) 24–26.
[19] J.H. Xu, G.S. Luo, S.W. Li, G.G. Chen, Shear force induced monodisperse droplet formation in a microfluidic device by controlling wetting properties, Lab. Chip 6 (2006) 131–136.
[20] A.M. Ganan-Calvo, J.M. Gordillo, Perfectly monodisperse microbubbling by capillary flow focusing, Phys. Rev. Lett. 87 (2001) 274501.
[21] A.M. Ganan-Calvo, Perfectly monodisperse microbubbling by capillary flow focusing: an alternate physical description and universal scaling, Phys. Rev. E 69 (2004) 027301.
[22] J.M. Gordillo, Z.D. Cheng, A.M. Ganan-Calvo, M. Marquez, D.A. Weitz, A new device for the generation of microbubbles, Phys. Fluids 16 (2004) 2828–2834.
[23] P. Garstecki, I. Gitlin, W. Diluzio, E. Kumacheva, H.A. Stone, G.M. Whitesides, Formation of monodisperse bubbles in a microfluidic flow-focusing device, Appl. Phys. Lett. 85 (2003) 2649–2651.
[24] P. Garstecki, H.A. Stone, G.M. Whitesides, Mechanism for flow-rate controlled breakup in confined geometries: a route to monodisperse emulsions, Phys. Rev. Lett. 94 (2005) 164501.
[25] J.H. Xu, S.W. Li, Y.J. Wang, G.S. Luo, Controllable gas–liquid phase flow patterns and monodisperse microbubbles in a microfluidic T-junction device, Appl. Phys. Lett. 88 (2006) 133506.
[26] M. Yasuno, S. Sugiura, S. Iwamoto, M. Nakajima, A. Shono, K. Satoh, Monodispersed microbubble formation using microchannel technique, AIChE J. 50 (2004) 3227–3233.
[27] J. Tan, J.H. Xu, S.W. Li, G.S. Luo, Drop dispenser in a cross-junction microfluidic device: scaling and mechanism of break-up, Chem. Eng. J. 136 (2008) 306–311.
[28] X.C. Yan, M.D. Luo, Surfactant in Interfacial chemistry, Chemical Industry Press, Beijing, 2005 p 53, p. 53.
[29] J.D. Tice, A.D. Lyon, R.F. Ismagilov, Effects of viscosity on drop formation and mixing in microfluidic channels, Anal. Chim. Acta 507 (2004) 73–77.
[30] S. van der Graaf, C.G.P.H. Schroën, R.G.M. van der Sman, R.M. Boom, J. Colloid Interface Sci. (2004) 277–456.